HOSTED BY

ELSEVIER

CrossMark

Available online at www.sciencedirect.com

ScienceDirect

Progress in Natural Science: Materials International 24 (2014) 354–363

Progress in Natural Science Materials International

www.elsevier.com/locate/pnsmi
www.sciencedirect.com

Original Research

Dissolution behavior of bioactive glass ceramics with different CaO/MgO ratios in SBF-K9 and r-SBF ☆

M.U. Hashmi[a,*], Saqlain A. Shah[b,c]

[a]Department of Applied Sciences, Superior University Lahore, Lahore 54000, Pakistan
[b]Department of Physics, FC College (A Chartered University), Lahore 54000, Pakistan
[c]Department of Material Science and Engineering, Washington University, St Louis, MO, USA

Received 23 April 2014; accepted 15 June 2014
Available online 27 August 2014

Abstract

In the present work, we studied dissolution behavior of three glass ceramics samples each having 34 SiO_2–14.5 P_2O_5–1 CaF_2–0.5 MgF_2 (%wt) and ratio of CaO/MgO varying from 11.5:1 to 1:11.5 in conventional SBF (SBF-K9) and revised SBF (r-SBF) that has ionic concentration exactly equal to that of human blood plasma. For that purpose, samples were immersed in fluids for different time periods upto 25 days. Thin film XRD analysis revealed the diffusive nature of the phases on the surfaces of samples after soaking for different time periods in r-SBF. It showed the poor precipitation and small thickness of the HCAp layer on the samples as compared to that in SBF-K9, thus indicating the fitness and sensitivity of r-SBF for in-vitro characterization of samples. AAS, FTIR and EDS revealed slow bonding rate on the surfaces of the samples in r-SBF than that in SBF-K9 that showed the dependence of bond formation on the composition of the materials as well as on the physiological fluid used for in-vitro characterization. The rate of HCAp formation was slower in r-SBF due to more competitive adsorption of CO_3^- ions to Ca and Mg ions owing to greater amount of CO_3^- in r-SBF than that in SBF-K9. It shows the importance of CO_3^- content in the physiological fluids for the in-vitro assessment of samples. So, r-SBF is recommended to be used for assessment of samples to clearly understand their behavior in-vivo.

Keywords: Dissolution behavior; SBF-K9; r-SBF

1. Introduction

Surrounding fluids play very important role in surface reactions and bonding to living bone [1] and soaking tests (in-vitro tests) give the appropriate idea about the chemical reactions in-vivo [2,3]. Distilled water and ionized water are the simplest physiological solutions for the in-vitro study but the behavior of materials in these solutions don't resemble to that of in-vivo because of deficiency in buffer capacity due to which pH of the solution changes. To overcome this problem, many physiological solutions with different buffers such as trimethylamines, phosphates and HCl etc. were introduced to maintain the pH between 7.2 and 7.4. In this field, work of Kokubo is worth mentioning. He developed a number of physiological solutions naming SBF-K1 to SBF-K9 with different buffers. Among all of these solutions, SBF-K9 was found to be the best solution for in-vitro study because all of its inorganic constituents are nearly equal to that of human blood plasma [4,5] whose results closely resembled to that of in-vivo [6–9]. He confirmed the concept that apatite layer always formed at the interface due to reaction of Ca_2^+, HPO_4^{-2} and OH^- ions in the fluid and the A–W glass ceramics material [10]. In 1999, Kim et al. investigated that HAp layer formed in conventional SBF(SBF-K9) is not similar to bone apatite, in its composition and structure, due to its lower CO_3^- ion concentration and higher Cl^- ion concentration than those of human blood plasma and in 2000, they clarified that HAp layer having the same composition and structure as of bone apatite, could be produced if a SBF is used whose ion concentration is exactly equal to that of human blood plasma or close to it [11,12].

*Corresponding author at: Department of Applied Sciences, Superior University Lahore, Lahore 54000, Pakistan. Tel.: +923334914120.
E-mail address: usmanhashmi06@hotmail.com (M.U. Hashmi).
Peer review under responsibility of Chinese Materials Research Society.

http://dx.doi.org/10.1016/j.pnsc.2014.07.004

In 2001, Jonasova et al. investigated effect of composition of SBF on the formation of HCAp layer. For this purpose, they tested SBFs with different concentration of HCO_3^- and Cl^- ions and suggested that the SBF that has HCO_3^- ions concentration close to that of human blood plasma could be more effective and appropriate for the in-vitro tests [13]. Upto 2003, a lot of research had been conducted on conventional SBF for in-vitro assessment of different materials but it was also a known fact that its ions concentration is not exactly equal to that of human blood plasma. Hence the structure and composition of HAp formed in it was also not equal to that of blood plasma [11,12]. Keeping it in mind, Oyane et al. prepared different types of physiological fluids (SBFs) named revised SBF (r-SBF), ionized SBF (i-SBF) and modified SBF (m-SBF). Among these SBFs, r-SBF had ion concentration exactly equal to that of human blood plasma, i-SBF had ions concentration equal to that of blood plasma in dissociated amounts whereas m-SBF had ions concentrations totally equal to that of human blood plasma except of HCO_3^- ions concentration. They recommended m-SBF for in-vitro assessment of bio-materials due to their longer stability and resemblance to human blood plasma [14,15] but its ion concentration was also not exactly equal to that of blood plasma. The use of r-SBF has also been proved to have exactly similar chemical composition as of natural bone [16,17]. In order to accelerate nucleation and precipitation of HCAp layer, many researchers took the idea to use the condensed solutions of C-SBF and r-SBF, even their condensation was increased upto 5 times the original one [18–28]. Later, it was found that, the higher the condensation of surrounding fluids, the greater the Ca/P ratio and the amount of carbonates in the layers due to which their resemblance to the natural bone became lower. So it was suggested to keep the condensation of the fluids as low as of natural bones in order to maintain the resemblance between precipitates and the bone [29]. Dissolution behavior of bioactive glass ceramics with different CaO/MgO ratios using SBF-K9 has already been investigated [30]. In the present work, dissolution behavior of bioactive glass ceramics with different CaO/MgO ratios was compared using SBF-K9 and r-SBF that has ions concentrations exactly equal to that of human blood plasma has been performed.

2. Experimental

2.1. Preparation of samples

Powders of three different compositions, 34 SiO_2–14.5 P_2O_5–1 CaF_2–0.5 MgF–46 CaO–4 MgO, 34 SiO_2–14.5 P_2O_5–1 CaF_2–0.5 MgF–25 CaO–25 MgO and 34 SiO_2–14.5 P_2O_5–1 CaF_2–0.5 MgF–4 CaO–46 MgO (%wt) were thoroughly mixed and melted under oxy-acetylene flame in a fire clay crucible. The melt of each composition was quenched in water to form three different glasses. Every glass was powdered using agate mortar and pestle for several hours. 5 wt% Polyvinyl Alcohol (PVA) was used as organic binder for compaction and powder was compacted under a pressure of 10 t/cm^2 in a hydraulic press. The glass compacts were sintered at 950 °C for 3 h to form glass ceramics, in a muffle furnace operating at the ramp rate of 5 °C/min. The samples were maintained at 700 °C for 1 h for the creation of nucleation sites before crystallization. The furnace was switched off at the end of each sintering process till the room temperature was achieved and samples were taken out.

The samples were named as G1, G2 and G3 respectively according to CaO/MgO ratios.

Table 1
Comparison of ion concentrations of different SBFs and human blood plasma (mmol/l).

	Na^+	Ca^+	K^+	Mg^{2+}	Cl^-	HCO_3^{2-}	HPO_4^{2-}	SO_4^{2-}
Kokubo SBF	142.0	2.5	5.0	1.5	109.0	27.0	1.0	0.5
Revised SBF	142.0	2.5	5.0	1.5	103.8	27.0	1.0	0.5
HB Plasma	142.0	2.5	5.0	1.5	103.8	27.0	1.0	0.5

Table 2
Reagents, purities and their amounts for preparation of 1000 ml SBFs.

Reagents	Purity (%)	Amount SBF-K9	Amount r-SBF
NaCl	99.5	8.036 g	5.403 g
$NaHCO_3$	99.5	0.352 g	0.740 g
Na_2CO_3	99.5		2.046 g
KCl	99.5	0.225 g	0.225 g
$K_2HPO_4 \cdot 3H_2O$	98	0.230 g	0.230 g
$MgCl_2 \cdot 6H_2O$	99	0.311 g	0.311 g
$CaCl_2$	95	0.293 g	0.293 g
Na_2SO_4	99	0.072 g	0.072 g
TRIS	99.5	6.063 g	11.928 g
HEPES	99.5		
1.0 M HCl		0.2 ml	
1.0 M NaOH			0.8 ml

2.2. Preparation of SBFs

To study the dissolution behavior of the samples in the in-vitro environment, SBF-K9 was selected as it is mostly used for in-vitro study and r-SBF as its ions concentrations is exactly equal to that of human blood plasma (Table 1).

2.2.1. Preparation of conventional SBF (SBF-K9)

For preparation of solution, NaCl, $NaHCO_3$, KCl, $K_2HPO_4 \cdot 3H_2O$, $MgCl_2 \cdot 6H_2O$, $CaCl_2$, Na_2SO_4 and $(CH_2OH)_3CNH_2$ respectively (Table 2) [31] were added in ultra pure water (in beaker) one by one by keeping it on a magnetic stirrer with heater at 37 °C. In order to avoid increase in pH of solution, the buffer agent $(CH_2OH)_3CNH_2$ (TRIS) was added in the solution little by little. By keeping the electrodes of pH meter in the solution, pH was adjusted at 7.4 by 1.0 M HCl.

2.2.2. Preparation of revised SBF (r-SBF)

For preparation of revised simulated body fluid, same reagents with the addition of Na_2CO_3 were used and the quantities of NaCl and $NaHCO_3$ were changed to a small extent as given in Table 2 and in order to avoid the increase in

pH of solution, 2-[4-(2-hydroxyethyl)-1-piperazinyl]ethanesulfonic acid (HEPES) was used and pH was adjusted at 7.4 by aqueous 1.0 M NaOH [14].

All the samples were put in the solution in different bottles and taken out after respective time periods and cleaned with distilled water and dried at 100 °C for two and half hours.

2.3. Characterization

It is assumed that decrease in P and Ca ions concentrations in the fluids show the spontaneous precipitation as well as instability of the fluids. So, in order to check the stabilities of fluids, the variation in ions concentration was studied by atomic absorption spectroscopy and checking the pH values of fluids in different time periods.

The pH of the fluids was measured before and after immersion of glass samples for various time periods using the pH meter (PCSIR manufactured).

In order to study the dissolution behavior of the samples in detail, concentrations of different ions in both the fluids, before and after immersion of glass samples for various time periods, were measured using atomic absorption spectroscopy (180-80, Hitachi).

The in-vitro test of bio-activity was carried out by immersing the glass ceramics samples in the fluids (mass/vol = .002 g/cm^3 at ambient temperature) for different time intervals. Structural characterization of the leached surface of in-vitro test glass ceramics samples was performed by thin film X-Ray Diffraction (Panalytical X'pert PRO MPD θ–θ X-Ray Diffractometer) using Cu $K\alpha 1$ radiation ($\lambda = 1.54056$ Å) by fixing the sample at an angle of 1° to the X-Ray beam.

Compositional analysis of the leached surface was performed by EDS (S-3700N, Hitachi, Japan).

In order to investigate the chemical reactions between the leached surface and SBF and to study the presence of bonds in the material, FTIR spectroscopy was used.

3. Results and discussion

3.1. Study of stability of SBF-K9 and revised SBF (r-SBF)

It is assumed that the spontaneous reduction of ions concentration from the fluids suggest the instability of the fluids. The stability of the physiological solutions was evaluated by investigating the dependence of variation of all the ions concentrations (particularly P and Ca) on time at ambient temperature. Fig. 1 shows almost no change in concentration of ions revealing the stability of SBF-K9 upto 30 days whereas, Fig. 2 indicates the decrease in the concentrations of Ca and P ions after 25 days showing instability of r-SBF after 25 days. Greater variation in pH values of r-SBF than that of SBF-K9 (Fig. 3) also confirmed the less stability of r-SBF as compared to that of SBF-K9 but it was confirmed that both fluids are strongly stable upto 25 days.

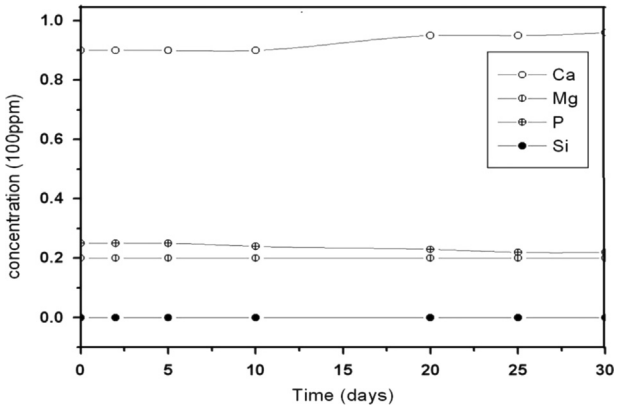

Fig. 1. Stability of SBF-K9.

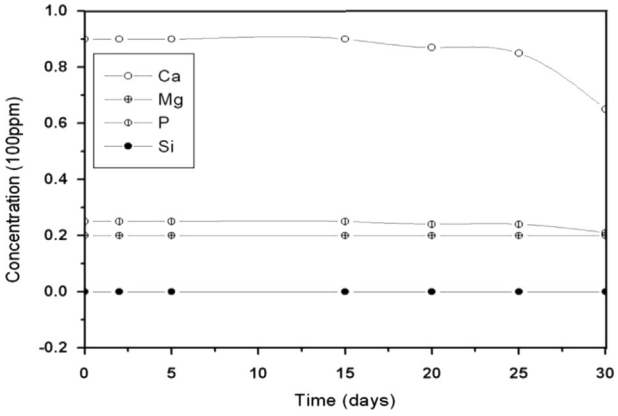

Fig. 2. Stability of r-SBF.

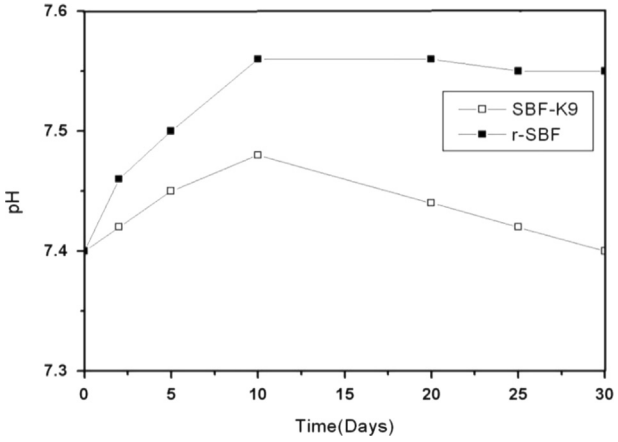

Fig. 3. pH of SBF-K9 and r-SBF.

3.2. XRD analysis

Fig. 4 gives a comparison of thin film XRD patterns of surfaces of G1, G2 and G3, soaked in SBF-K9 and r-SBF for 2, 5, 10, 20 and 25 days.

It is clear from the figure that in SBF-K9, HCAp phase appears on the surface of G1 after 5 days revealing bond formation after 2 days as discussed earlier whereas in r-SBF, HCAp phase appears after 10 days indicating the bond

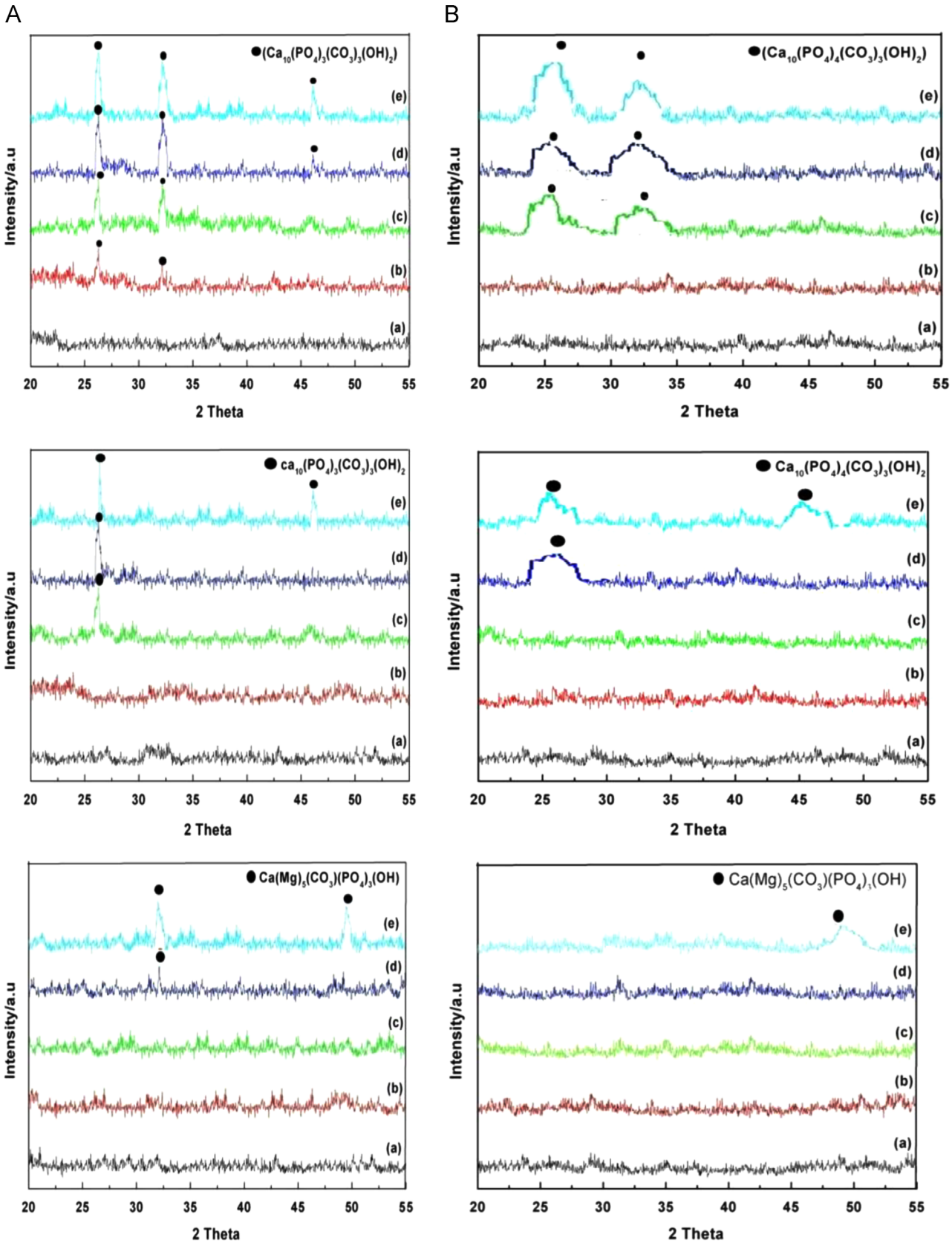

Fig. 4. Thin film XRD patterns of G1, G2 and G3 (up to down respectively) in (A) SBF-K9 and (B) r-SBF after different immersion periods, (a) 2 days (b) 5 days (c) 10 days (d) 20 days (e) 25 days.

formation on the surface of G1 after 5 days instead of 2 days due to greater amount of CO_3^- ion in r-SBF that has ability to suppress the formation of HCAp due to its ability to confine the adsorption of phosphate ions on the surface of the samples owing to aggressive adsorption of HCO_3^- to Ca_{2+} ions. Figure also shows the diffusive nature of phases in r-SBF that indicates the poor crystallinity of HCAp phases and small thickness of the precipitated layer on the samples.

Similarly, HCAp phase appears on surface of G2 after 10 days, in case of SBF-K9, indicating the bond formation after 5 days whereas in r-SBF, HCAp phase was appeared after 20 days indicating bond formation after 10 days instead of 5 days due to greater amount of MgO in G2 as well as higher amount of CO_3^- ions concentration in r-SBF. The intensities of these phases then gradually increase with the passage of immersion time as shown in figure.

Fig. 4 reveals the appearance of Mg-HCAp (Magnesium Hydroxycarbonate Apatite) phase on the surface of G3 after 20 days, in case of SBF-K9, indicating the bond formation after 10 days whereas small crystalline phase of Mg-HCAp was observed on the surface of G3 after 25 days immersion in r-SBF, revealing bond formation after 20 days. This delay in bond formation may be due to very large amount of MgO in G3 that may cause more aggressive adsorption of HCO_3^- ions to Mg ions owing to greater amount of CO_3 in r-SBF.

In spite of the fact that bond formation in r-SBF is slower as compared to SBF-K9, it may be suggested that in-vitro assessment of the samples in r-SBF could enable the more sensitive testing of bio-materials. Moreover, during the interaction with human blood plasma, the creation of HCAp could be awaited rather than pure hydroxyapatite precipitation. Therefore the content of carbonate ions in the solution can be important for the plausibility of in-vitro test. Assessment of samples in r-SBF could clearly indicate the timing of bond formation and behavior of samples in-vivo because its ion concentration is exactly equal to human blood plasma. So r-SBF should be used for assessment of samples to clearly understand their behavior in-vivo. However its drawback is its low stability (25 days) due to which it is only useful for the in-vitro characterization of the samples upto 25 days.

3.3. Atomic absorption spectroscopy

Atomic absorption spectroscopy was used to measure the concentrations of Ca, P, Si and Mg ions in SBF-K9 and r-SBF to study the dissolution behavior of samples in more detail.

It is found that in G1, concentration of Ca and Mg ions increases in SBF-K9 in first 2 days (Fig. 5) whereas in r-SBF, the increase of Ca and Mg ions is upto 5 days. This difference in increase of ion concentrations in both the fluids is attributed to difference in concentration of HCO_3^- ions in both the fluids. The increase in Ca and Mg ions in both the fluids is attributed to exchange of Ca or Mg ions from G1 with H^+ or H_3O^+ ions from the fluids and as a result, silanol group (Si–OH) is formed on the glass surface due to reaction of Si with OH^- ions that act as nucleation agent for HCAp formation. After 2 days, concentration of Ca and P ions decrease continuously in SBF-K9 whereas in r-SBF, decrease in concentrations of Ca and P ions start after 5 days. This time difference in decrement of Ca and P ions between both the fluids, that indicates the HCAp formation on G1, also corresponds to difference in HCO_3^- ions concentration in the fluids because it is considered that, the higher the HCO_3^- ions concentration in the fluid, the lower the phosphate adsorption on the surface of sample due to its (HCO_3^- ion's) competitive adsorption to Ca^{2+} ions that causes suppression to the bond formation on the samples. Si ion concentration is found to be increased very fast in the earlier days of immersion and then increase gradually in both the fluids, however, increase in Si concentration is slightly slower in SBF-K9 as compared to r-SBF. pH values of fluids are found to be increased with Si concentration showing direct relationship with each other in both the fluids.

In G2, the behavior of increase of Ca in r-SBF is found to be more complicated as compared to G1 and G3. Ca ions in r-SBF increase up to 5 days, then decrease up to 10 days and then again increase up to 20 days and then decreases showing HCAp formation on G2 after 10 days as conformed by other characterization techniques. Whereas in SBF-K9, Ca increase up to 5 days and then decrease continuously thereafter showing HCAp formation after 5 days. However behavior of P ions concentrations is straight forward in both the fluids. It increases upto 5 days in SBF-K9 following decrement in its concentration and increases upto 10 days in r-SBF then decreases, confirming HCAp formation on G2 after 5 days in case of SBF-K9 and after 10 days in r-SBF. The delay in bone bonding mechanism of G2 in case of r-SBF may be due to higher amount of CO_3^- ions concentration in r-SBF as compared to SBF-K9. It shows the dependence of bond formation on composition of the materials and also on the physiological fluid used for in-vitro characterization. Si ion concentration show linear relationship with pH as in G1 and increases quickly in earlier days and then gradually in the upcoming days. The increase of Si concentration in the fluids is not as fast as in case of G1 due to less CaO/MgO ratio.

In G3, Ca, P and Mg ions go on increasing in r-SBF upto 20 days and then decrease. It showed small phase formation of Mg-HCAp on sample after 20 days whereas in SBF-K9, Ca, P and Mg ions are found to be increased upto 10 days and then decrease, showing Mg-HCAp formation on surface of G3 after 10 days, as conformed by other characterization techniques. In this case also, change in Si concentration is directly related to pH indicating the saturation of Si component in the SBFs. Variations in pH values of SBF-K9 and r-SBF after immersion of G1, G2 and G3, for different time periods is shown in Fig. 6.

3.4. Fourier transform infrared spectroscopy

Fig. 7 shows the FTIR graphs of G1, G2 and G3 in SBF-K9 and r-SBF respectively, before immersion, and 2, 5, 10, 20 and 25 days after immersion.

In G1, the vibrational bands: $Si–O–Si_{stretch}$ (1085 cm^{-1}), $Si–O_{bend}$ (800 cm^{-1}) and $Si–O–Si_{bend}$ (460 cm^{-1}) decrease frequently in the earlier days of immersion and then decrease

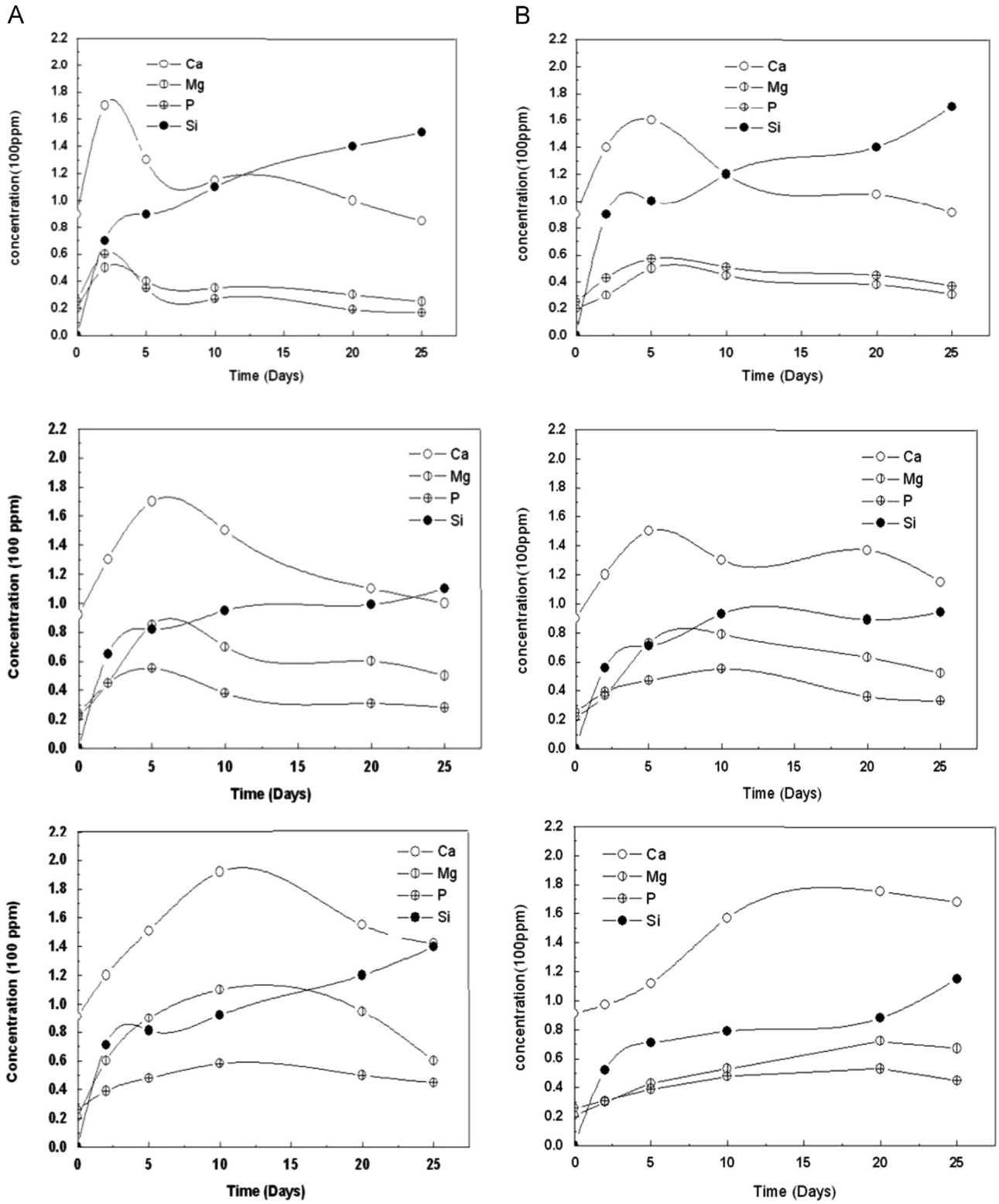

Fig. 5. Variation of Ions concentration in (A) SBF-K9 and (B) r-SBF, in case of G1, G2 and G3 (up to down respectively) with different soaking times.

gradually with the passage of immersion time that correspond to the increasing dissolution of wollastonite into Ca^{2+} ions and SiO_2 in SBF-K9 and the same behavior was observed in r-SBF. In SBF-K9, peak intensities of $P–O_{stretch}$ vibrational modes at 1038 cm^{-1} and 960 cm^{-1} and $P–O_{bend}$ mode at 570 cm^{-1} decrease upto 2 days and then increases with the passage of immersion time indicating the growing crystallization of biological hydroxycarbonate apatite (HCAp) phase

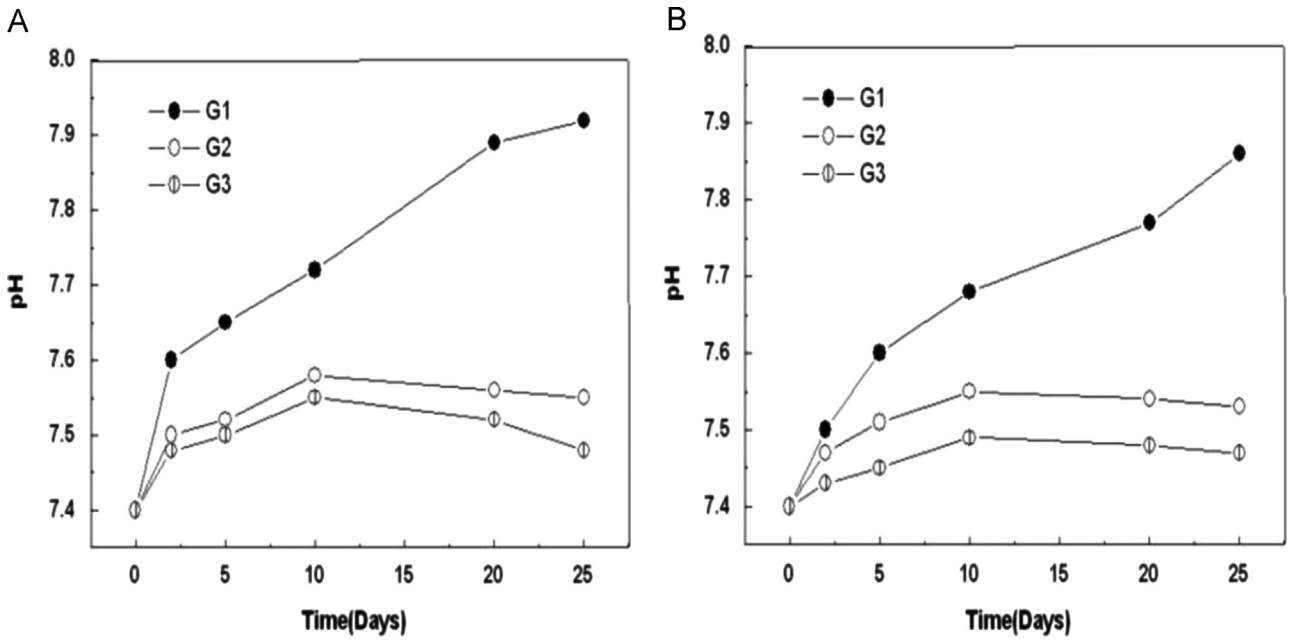

Fig. 6. Variations in pH values of (A) SBF-K9 and (B) r-SBF after immersion of G1, G2 and G3 for different time periods.

on G1 whereas in r-SBF, these modes were found to be decreased upto 5 days and then increase showing the slightly less bioactivity of G1 in r-SBF as compared to that in SBF-K9 due to high HCO_3^- concentrations in r-SBF. The sequence of reactions in SBF is such that release of SiO_2 is followed by the development of silanols (Si–OH) at the material solution interface and eventually by the condensation and repolymerization of SiO_2 rich layer at the material surface. Silica rich layer provides the nucleation sites for the Ca^{2+} and $(PO_4)^{2-}$ ions to build up from the SBF on the material surface to precipitate into biological HCAp. The bands located at 1444 cm^{-1} and 870 cm^{-1} can be assigned to C–$O_{stretch}$ vibration mode of CO_3^{2-} [32] which are appeared after 2 days in SBF-K9 and after 5 days in r-SBF indicating the HCAp formation on the surface of G1 after 2 days, when immersed in SBF-K9 and after 5 days in case of r-SBF. These bands signify the absorption of carbonate anions from the SBFs in hydroxyapatite crystal lattice to form biological HCAp.

In G2, the vibrational bands: Si–O–$Si_{stretch}$ (1085 cm^{-1}), Si–O_{bend} (800 cm^{-1}) and Si–O–Si_{bend} (460 cm^{-1}) shows the same behavior as in G1, in both the fluids. In SBF-K9, peak intensites of P-$O_{stretch}$ vibrational modes at 1038 cm^{-1} and 960 cm^{-1} and P–O_{bend} mode at 570 cm^{-1} decrease upto 5 days and then increases with the passage of immersion time indicating the growing crystallization of biological hydroxycarbonate apatite (HCAp) phase on G2 whereas in r-SBF, these bonds were found to be decreased upto 10 days and then increase continuously showing HCAp formation after 10 days as conformed by other characterization techniques. It also shows lesser bioactivity of G2 in r-SBF as compared to that in SBF-K9 due to high HCO_3^- concentrations in r-SBF as also conformed by Atomic Absorption Spectroscopy (AAS) analysis. This delay in bone bonding mechanism may be attributed to equal and high concentration of CaO and MgO in G2 due exchange of Ca or Mg ions from G2 with H^+ or H_3O^+ ions from SBF may become resistive by the help of two factors: one, greater amount of Mg in G2 that has ability to suppress the bone bonding mechanism, two, greater amount of HCO_3^- concentration in r-SBF that also resist the bond formation due to which silanol group (Si–OH) formation is delayed on the glass surface owing to reaction of Si with OH^- ions that act as nucleation agent for HCAp formation. The bands of CO_3^{2-} located at 1444 cm^{-1} and 870 cm^{-1} are appeared after 10 days in SBF-K9 and after 20 days in r-SBF, again indicating the delayed HCAp formation in r-SBF as conformed by other characterization techniques.

In G3, bands: Si–O–$Si_{stretch}$ (1085 cm^{-1}), Si–O_{bend} (800 cm^{-1}) and Si–O–Si_{bend} (460 cm^{-1}) shows the same behavior as in G1 and G2, in both the fluids. In SBF-K9, peak intensities of P–$O_{stretch}$ vibrational modes at 1038 cm^{-1} and 960 cm^{-1} and P–O_{bend} mode at 570 cm^{-1} and Mg–OH modes at 570 cm^{-1} decrease upto 20 days and then increases with the passage of immersion time and besides, the C–O bands appear at 870 and 1440 cm^{-1} indicating the growing crystallization of biological Mg-hydroxycarbonate apatite (Mg-HCAP) phase on G3 whereas in r-SBF, these modes go on decreasing upto 20 days and then increase. C–O band appears at 1440 cm^{-1} after 25 days indicating the appearance of Mg-HCAp phase after 25 days as conformed by other characterization techniques that is also due to very high amount of MgO in G3 as well as high HCO_3^- ion concentration in r-SBF.

3.5. EDS analysis

Tables 3–5 show the intensities of EDS spectrum for materials components of G1, G2 and G3 respectively, before and after immersion in SBF-K9 and r-SBF for different days. Table 3 shows that after immersion of G1 in SBF-K9 for 2

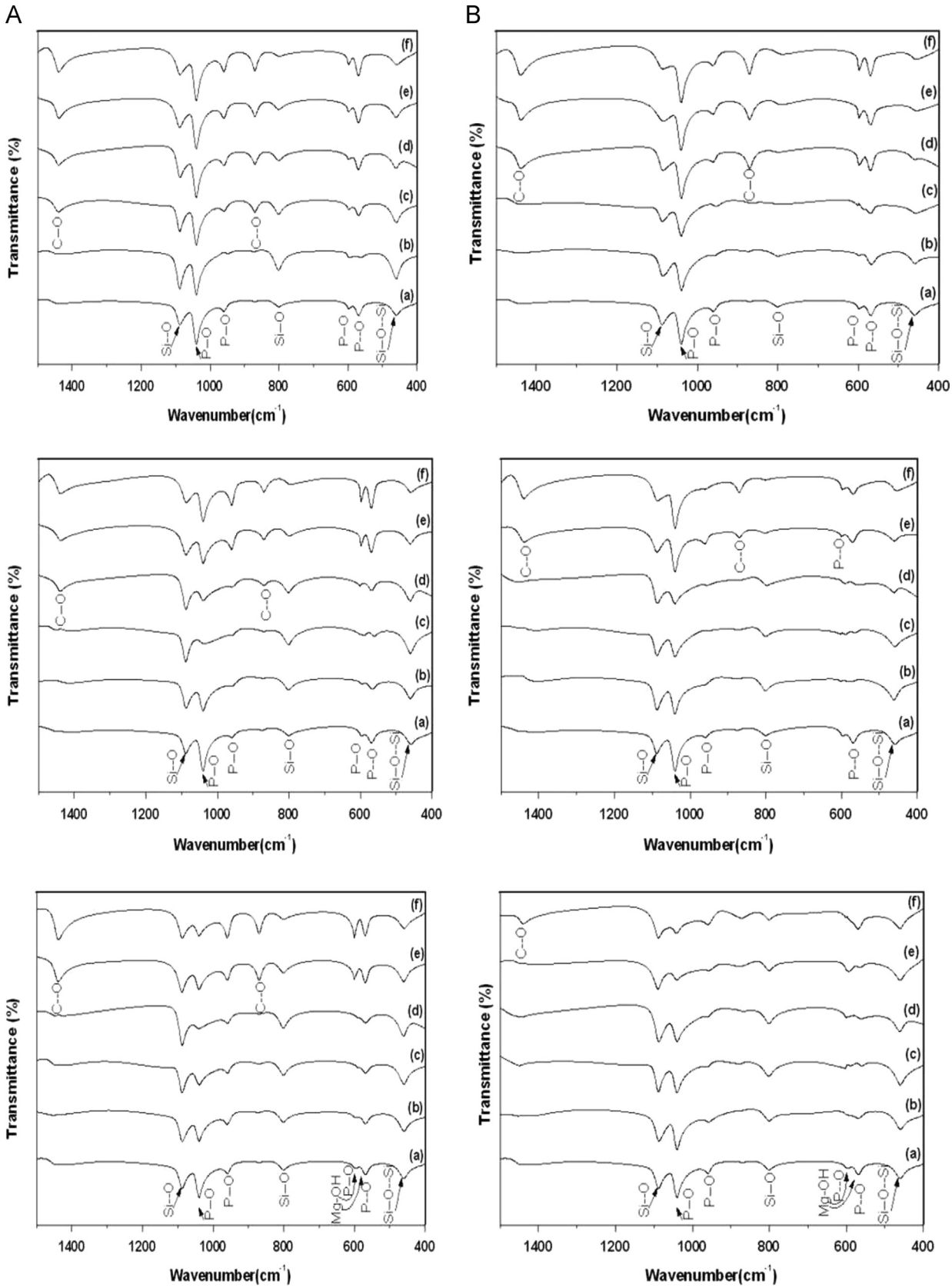

Fig. 7. FTIR patterns of G1, G2 and G3 (up to down respectively) in (A) SBF-K9 and (B) r-SBF for different immersion periods (a) before immersion (b) after 2 days immersion (c) after 5 days immersion (d) after 10 days immersion (e) after 20 days immersion (f) after 25 days immersion.

Table 3
The table of intensities of EDS spectrum of materials components of G1 before and after immersion in r-SBF and SBF-K9 (a.u).

	Ca		P		Si		Ca		O		C		Mg	
	SBF-K9	r-SBF	SBF-K9	r-SBF	SBF-K9	r-SBF	SBF-K9	r-SBF	SBF-K9	r-SBF	SBF-K9	r-SBF	SBF-K9	r-SBF
Before immersion	645	645	707	707	578	578	495	495	335	335	0	0	0	0
After 2 days	599	632	635	696	674	599	463	489	394	367	0	0	0	0
After 5 days	638	617	700	675	622	612	495	470	392	387	87	0	0	0
After 10 days	663	652	732	713	590	541	516	519	396	403	105	83	0	0
After 20 days	665	671	753	739	580	532	523	531	390	381	114	123	0	0
After 25 days	674	699	769	767	555	524	527	589	364	374	155	161	0	0

Table 4
The table of intensities of EDS spectrum of materials components of G2, before and after immersion in r-SBF and SBF-K9 (a.u).

	Ca		P		Si		Ca		O		C		Mg	
	SBF-K9	r-SBF	SBF-K9	r-SBF	SBF-K9	r-SBF	SBF-K9	r-SBF	SBF-K9	r-SBF	SBF-K9	r-SBF	SBF-K9	r-SBF
Before immersion	592	592	693	693	580	580	424	424	348	348	0	0	0	0
After 2 days	555	561	612	587	610	613	390	399	374	381	0	0	0	0
After 5 days	502	541	486	571	638	627	323	367	399	387	0	0	0	0
After 10 days	537	529	534	539	624	648	346	352	381	399	52	0	0	0
After 20 days	596	570	626	619	578	551	385	403	355	348	93	63	0	0
After 25 days	619	673	684	702	555	532	415	471	337	339	105	113	0	0

Table 5
The table of intensities of EDS spectrum of materials components of G3, before and after immersion in r-SBF and SBF-K9 (a.u).

	Ca		P		Si		Ca		O		C		Mg	
	SBF-K9	r-SBF	SBF-K9	r-SBF	SBF-K9	r-SBF	SBF-K9	r-SBF	SBF-K9	r-SBF	SBF-K9	r-SBF	SBF-K9	r-SBF
Before immersion	502	502	587	587	590	590	413	413	351	351	0	0	82	82
After 2 days	440	463	486	567	605	603	420	387	362	358	0	0	70	73
After 5 days	376	437	385	532	624	627	236	352	387	373	0	0	61	66
After 10 days	316	423	261	503	645	643	178	321	399	381	0	0	70	61
After 20 days	413	393	401	481	605	671	231	299	369	385	54	0	80	52
After 25 days	500	472	537	519	576	603	371	353	346	364	77	67	96	86

days, EDS illustrates the gradual decrease in Ca and P ions from G1 due to their exchange with H^+ or H_3O^+ ions from SBF and after that, intensities of EDS spectrums show the continuous increase in P and Ca ions concentration and presence of C in G1 indicating the formation of HCAp layer as conformed by other characterization techniques. Whereas EDS analysis of G1 after immersion in SBF-K9 indicates the decrease in Ca and P ions upto 5 days following the increase in the concentrations of these ions in the upcoming days and appearance of C after 5 days indicates the HCAp formation after 5 days instead of 2 days due to greater amount of HCO_3^- content in r-SBF that plays an important role in delaying the bond formation.

Table 4 shows that in case of G2, concentration of Ca and P decreases gradually up to 5 days in case of SBF-K9 and after that their concentration start increasing that is attributed to formation of HCAp layer whereas in case of r-SBF, Ca and P ions on G2 are found to be decreased upto 10 days following the increase in these ions concentration revealing the formation of the HCAp after 10 days.

In G3 (Table 5), concentration of Ca and P decreases continuously up to 10 days and after that their concentration starts increasing and small intensities of Mg also appears due to large amount of Mg in G3 that is attributed to formation of Mg-hydroxycarbonate apatite layer as conformed by XRD results. Whereas in case of r-SBF, concentration of Ca and P goes on decreasing from G3 up to 20 days and then increases revealing Mg-HCAp phase formation on G3 after 20 days immersion.

4. Conclusion

(1)- A comparative study of in-vitro dissolution behavior was performed by soaking the samples in SBF-K9 and r-SBF whose ion concentration is exactly equal to that of human blood plasma, for different time periods.

(2)- Thin film XRD analysis revealed the diffusive nature of phases on the surfaces of the samples after soaking for different time periods in r-SBF that showed the poor crystallinity of HCAp phases and small thickness of the precipitated layer on the samples as compared to that in SBF-K9. It indicates the fitness and sensitivity of r-SBF for in-vitro characterization of biological samples.

(3)- AAS, FTIR and EDS revealed slow bonding rate on the surfaces of samples and complicated dissolution behavior of G2 in r-SBF than that in SBF-K9. It shows the dependence of bond formation on composition of the materials as well as on the physiological fluid used for in-vitro characterization.

(4)- The rate of HCAp formation was found to be slower in r-SBF, as conformed by different characterization techniques, due to more competitive adsorption of CO_3^{2-} ions to Ca and Mg ions owing to greater amount of CO_3^{2-} in it than that in SBF-K9. It revealed the importance of CO_3^{2-} content in the physiological fluids for the in-vitro assessment of samples.

(5)- Assessment of samples in r-SBF could clearly indicate the timing of bond formation and behavior of samples in-vivo because its ion concentration is exactly equal to human blood plasma so r-SBF should be recommended for assessment of samples to clearly understand their behavior in-vivo.

(6)- The negative aspect of r-SBF is its low stability (25 days), due to which, it can only be used for in-vitro characterization of samples upto 25 days. After that, it is much complicated to distinguish between biological HCAp layer and its own spontaneously developed layer on its surface.

Acknowledgements

Authors acknowledge the cooperation of Dr. Riaz Ahmad, chairman of the Physics department, GC University Lahore and support of Higher Education Commission, Government of Pakistan. Authors are grateful to Dr. Muhammad Mujahid, Department of Chemical and Materials Engineering, National University of Science & Technology (NUST) and Dr. Abdul Majeed, Brooklyn Hospital Centre, Brooklyn NY U.S.A, for their technical assistance.

References

[1] C. Ohtsuki, H. Kushitani, T. Kokubo, S. Kotani, T. Yamamuro, J. Biomed. Mater. Res. 25 (11) (1991) 1363–1370.
[2] Y.-R. Cai, L. Zhou, Y.-M. Zhang, J.-H. Wei, C.K. Yu, G. Xuebao, J. Mater. Sci. Eng. 23 (6) (2005) 792–795.
[3] R. Xin, L. Yang, C. Jiyong, Z. Qiyi, Biomaterials 26 (2005) 6477–6486.
[4] A.R. Boccaccini, J.E. Gough, Tissue Engineering using Ceramics and Polymers, CRC press New York, Washington, WP Ltd., Cambridge England, 2007, p. 19.
[5] T. Kokubo, H. Kushitani, C. Ohtsuki, S. Sakka, J. Mater. Sci.—Mater. Med. 3.2 (1992) 79–83.
[6] I. Barrios de Arenas, C. Schattner, M. Vásquez, Ceram. Int. 32 (2006) 515–520.
[7] S. Hayakawa, K. Tsuru, C. Ohtsuki, A. Osaka, 29 Si and 31P MAS-NMR analysis of apatite formation on sodium silicate glass in a simulated body fluid, in: Proceedings of International Congress on Glass, 18th, San Francisco, CA, United States, (1998), pp. 1565–1570.
[8] A. Saranti, I. Koutselas, M.A. Karakassides, J. Non-Cryst. Solids (2006) 390–398.
[9] J. Clément, L. Ekeberg, S. Martinez, M.P. Ginebra, F.J. Gil, J.A. Planell, Bioceramic 11 (1998) 141–144.
[10] T. Kokubo, H. Kushitani, S. Sakka, T. Kitsugi, T. Yamamuro, J. Mater. Sci.—Mater. Med. 4 (1993) 127–131.
[11] H.M. Kim, K. Kishimoto, F. Miyaji, T. Kokubo, T. Yao, Y. Suetsugu, J. Tanaka, T. Nakamura, J. Biomed. Mater. Res. 46 (1999) 228–235.
[12] H.M. Kim, K. Kishimoto, F. Miyaji, T. Kokubo, T. Yao, Y. Suetsugu, J. Tanaka, T. Nakamura, J. Mater. Sci.—Mater. Med. 11 (2000) 421–426.
[13] A. Helebrant, L. Jonasova, L. Sanda, Ceram. Silik. 46 (1) (2002) 9–14.
[14] A. Oyane, H. Kim, T. Furuya, T. Kokubo, T. Miyazaki, T. Nakamura, J. Biomed. Mater. Res. Part A 65 (2003) 188–195.
[15] A. Oyane, K. Onuma, A. Ito, H.-M. Kim, T. Kokubo, T. Nakamura, J. Biomed. Mater. Res. Part A 64 (2) (2003) 339–348.
[16] H.-M. Kim, T. Furuya, T. Kokubo, T. Miyazaki, T. Nakamura, Composition of apatite produced in simulated body fluids, in: S. Brown, I.C. Clarke, P. Williams (Eds.), Bioceramics 14, 218 –220, Trans Tech Publications, Switzerland, 2002, pp. 621–624 (Key Eng Mater).
[17] H. Kaneko, M. Uchida, H.-M. Kim, T. Kokubo, T. Nakamura, Process of apatite formation induced by anatase on titanium metal in simulated body fluid, in: S. Brown, I.C. Clarke, P. Williams (Eds.), Bioceramics 14, 218 –220, Trans Tech Publications, Switzerland, 2002, pp. 649–652 (Key Eng Mater).
[18] H.K. Varma, Y. Yokogawa, F.F. Espinosa, Y. Kawamoto, K. Nishizawa, F. Nagata, T. Kameyama, Biomaterials 20 (1999) 879–884.
[19] Y.E. Greish, P.W. Brown., J. Biomed. Mater. Res. 52 (2000) 687–694.
[20] H. Takadama, H.-M. Kim, T. Kokubo, T. Nakamura, J. Biomed. Mater. Res. 57 (2001) 441–448.
[21] S.H. Rhee, J. Tanaka, Biomaterials 20 (1999) 2155–2160.
[22] F. Miyaji, H.-M. Kim, S. Handa, T. Kokubo, T. Nakamura, Biomaterials 20 (1999) 913–919.
[23] H.-M. Kim, K. Kishimoto, F. Miyaji, T. Kokubo, T. Yao, Y. Suetsugu, J. Tanaka, T. Nakamura, J. Biomed. Mater. Res. 46 (1999) 228–235.
[24] H.-M. Kim, K. Kishimoto, F. Miyaji, T. Kokubo, T. Yao, Y. Suetsugu, J. Tanaka, T. Nakamura, J. Mater. Sci.—Mater. Med. 11 (2000) 421–426.
[25] A. Bigi, E. Boanini, S. Panzavolta, N. Roveri, Biomacromolecules 1 (2000) 752–756.
[26] F. Barrere, C.A. van Blitterswijk, K. de Groot, P. Layrolle, Biomaterials 23 (2002) 1921–1930.
[27] F. Barrere, C.A. van Blitterswijk, K. de Groot, P. Layrolle, Biomaterials 23 (2002) 2211–2220.
[28] P. Habibovic, F. Barrere, C.A. van Blitterswijk, K. de Groot, P. Layrolle, J. Am. Ceram. Soc. 85 (2002) 517–522.
[29] I. Dorozhkina, S.V. Dorozhkin, Research Institute of Fertilizers, Kudrinskaja sq.-155, 123242 Moscow D-242, Russia Received 21 January 2003; Revised 20 March 2003; Accepted 1 April 2003.
[30] M.U. Hashmi, S.A. Shah, S. Alam, A. Shamim, Ceram. Silik. 54 (1) (2010) 8–13.
[31] X. Li, A. Ito, X. Wang, R.Z. LeGeros, Acta Biomaterealia 5 (2009) 508.
[32] J.M. Oliveira, R.N. Correia, M.H. Fernandes, Biomaterials 23 (2002) 371–379.